



King Saud University  
Arabian Journal of Chemistry

[www.ksu.edu.sa](http://www.ksu.edu.sa)  
[www.sciencedirect.com](http://www.sciencedirect.com)



## ORIGINAL ARTICLE

# RKKY magnetic interactions in chemically synthesized $Zn_{0.95-x}Fe_{0.05}Al_xO$ ( $x = 0, 0.03, 0.05, 0.07$ ) nanocrystallites



Shahid M. Ramay<sup>a</sup>, Murtaza Saleem<sup>c</sup>, Shahid Atiq<sup>c</sup>, Saadat A. Siddiqi<sup>d</sup>,  
Muhammad Imran<sup>a</sup>, Yousef S. Al-Zeghayer<sup>a,b</sup>, Abdulrhman S. Al-Awadi<sup>a</sup>,  
Sajjad Haider<sup>a</sup>, Asif Mahmood<sup>a,\*</sup>

<sup>a</sup> Department of Chemical Engineering, College of Engineering, King Saud University, P.O. Box 800, Riyadh 11421, Saudi Arabia

<sup>b</sup> Supervisor of Industrial Catalysts Research Chair (KSU), Saudi Arabia

<sup>c</sup> Centre for Solid State Physics, University of the Punjab, Quaid-e-Azam Campus, Lahore 54590, Pakistan

<sup>d</sup> Interdisciplinary Research Centre in Biomedical Materials, COMSATS Institute of Information Technology, Defence Road, Off Raiwind Road, Lahore, Pakistan

Received 6 November 2012; accepted 20 February 2013

Available online 5 March 2013

## KEYWORDS

Diluted magnetic semiconductors;  
Auto-combustion;  
Magnetic properties;  
RKKY interactions

**Abstract** Chemically derived auto-combustion technique is employed to synthesize the  $Zn_{0.95-x}Fe_{0.05}Al_xO$  ( $x = 0, 0.03, 0.05, 0.07$ ) nano-crystallites. The salient similarities between variations in lattice parameters, crystallite size, morphology, electrical resistivity and saturation magnetization designated a strong association between these properties. X-ray diffraction studies of all compositions revealed the phase pure wurtzite crystal structure with space group  $P6_3mc$ . The lattice parameters and crystallite size are changed with doping of Al attributed to the diversity in the size of ionic radii. Scanning electron micrographs revealed that Al doping affects the size and shape of grains in synthesized compositions. Temperature dependent electrical resistivity shows a decreased trend with the rise of temperature, confirming the semiconducting nature of compositions. The lower resistivity and enhanced saturation magnetization values in Al doped compositions correspond to the increase in density of carriers. Carrier mediated RKKY interactions are found to enhance magnetization.

© 2013 King Saud University. Production and hosting by Elsevier B.V. This is an open access article under the CC BY-NC-ND license (<http://creativecommons.org/licenses/by-nc-nd/3.0/>).

\* Corresponding author. Tel.: +966 535764026.

E-mail addresses: [ahayat@ksu.edu.sa](mailto:ahayat@ksu.edu.sa), [asifawan@kaist.ac.kr](mailto:asifawan@kaist.ac.kr) (A. Mahmood).

Peer review under responsibility of King Saud University.



Production and hosting by Elsevier

## 1. Introduction

Diluted magnetic semiconductors (DMSs) have recently gained much interest due to the availability of data processing and storage facilities in single materials (Saleem et al., 2011a; Wolf et al., 2001). DMS materials are prospective candidates for applications in electronics technology involving the spin

<http://dx.doi.org/10.1016/j.arabjc.2013.02.017>

1878-5352 © 2013 King Saud University. Production and hosting by Elsevier B.V.

This is an open access article under the CC BY-NC-ND license (<http://creativecommons.org/licenses/by-nc-nd/3.0/>).

degree of freedom of electrons (Wolf et al., 2001; Fukumura et al., 2004; Pearton et al., 2005). The main objective is to fabricate crystalline materials with room temperature (RT) ferromagnetism that can make it possible to establish the spin based technology. An extensive research work has been performed for preparation and characterization of transition metal (TMs) doped oxide semiconducting materials like ZnO,  $\text{TiO}_2$ ,  $\text{SnO}_2$ , etc. (Coe et al., 2004, 2005; Hong et al., 2004). In II–VI oxide semiconducting materials, TM (Mn, Ni, Co and Fe) doped ZnO has attracted a great deal of interest theoretically as well as experimentally, due to its promising semiconducting and RT ferromagnetic properties (Ahmed et al., 2012a,b; Saleem et al., 2012). It was observed that ferromagnetic behavior in these materials strongly associated with crystal structure, grain size and concentration of dopants (Gupta et al., 2007; Venkatesan et al., 2004). The origin of ferromagnetism in DMSs is still a subject of controversy among research community. It was reported that secondary phases and clusters of TMs might be responsible for RT ferromagnetism in TM doped ZnO (Kim et al., 2002; Park et al., 2004). The ferromagnetic behavior in pure ZnO without doping of TMs was also observed by some groups (Ahmed et al., 2011a,b). According to most recent reports about DMSs, ferromagnetic interactions might be associated with vacancy induced mechanism (Yu et al., 2010), hole mediated Zener field model, (Yang et al., 2009) and carrier (electrons) mediated Rudermann Kittel Kasuaya Yoshida (RKKY) interactions (Tong et al., 2010; Saleem et al., 2011b). Therefore, careful studies with phase pure high quality DMS compositions are needed to resolve this controversy. Though, there are only few reports regarding the correlation between structural, morphological and magnetic properties for Fe doped ZnO nanocrystallites in this research work, Fe doped ZnO nanocrystallites have been synthesized using a sol–gel derived auto-combustion technique with co-doping of Al content (at 3, 5 and 7%). The substitution of  $\text{Al}^{3+}$  content at  $\text{Zn}^{2+}$  sites would significantly enhance the concentration of carriers in host structure. Carrier mediated RKKY mechanism possibly responsible for RT ferromagnetism in phase pure TMs doped ZnO based DMSs can be studied in this way by varying the concentration of Al content.

## 2. Experimental

In order to synthesize  $\text{Zn}_{0.95}\text{Fe}_{0.05}\text{Al}_x\text{O}$  ( $x = 0, 0.03, 0.05, 0.07$ ) nanocrystallites, stoichiometric calculated ratios of analytical grade Zn nitrate [ $\text{Zn}(\text{NO}_3)_2 \cdot 6\text{H}_2\text{O}$ ], Fe nitrate [ $\text{Fe}(\text{NO}_3)_3 \cdot 6\text{H}_2\text{O}$ ], Al nitrate [ $\text{Al}(\text{NO}_3)_3 \cdot 6\text{H}_2\text{O}$ ] and citric acid ( $\text{C}_6\text{H}_8\text{O}_7$ ) were dissolved in 75 ml distilled water. Metal nitrates to citric acid ratios were taken as 1:2. Citric acid was used here as fuel agent. The estimated pH of the initial solution was measured at 3.5. This prepared solution was vigorously stirred and heated at 200 °C. The xerogel was attained in a short time of 2 h. Then, the temperature was raised to 300 °C and xerogel was transformed into fine particles by an intense self propagated exothermic auto-combustion reaction. As-synthesized resulting powder compositions were characterized using X-ray diffraction (XRD), scanning electron microscope (SEM), two point probe electrical resistivity setup, and physical property measurement setup (PPMS) for various properties' measurements. Rigaku, ultm IV XRD was used

to explore the structural features and phase identification at 40 kV and 40 mA with  $\text{Cu K}\alpha_1$  radiation ( $\lambda = 1.540598 \text{ \AA}$ ) and a step scan size of 0.03. Jeol JSM 6610 V SEM was operated at 20 kV in the SEI mode in order to observe morphology of the samples. The Quantum Design PPMS was employed at  $\pm 13 \text{ kO}$  to study the magnetic properties of the samples. The powdered samples were pelletized and sintered using Apex hydraulic and muffle furnace for electrical resistivity measurements by a two point probe measurement setup.

## 3. Results and discussion

### 3.1. X-ray diffraction analysis

Fig. 1 shows the XRD patterns of  $\text{Zn}_{0.95}\text{Fe}_{0.05}\text{Al}_x\text{O}$  ( $x = 0, 0.03, 0.05, 0.07$ ) nanocrystallites. ZnO is a fairly moderate semiconductor material, as it retains its wurtzite hexagonal crystal structure while doped with diluted amounts of TM elements (Pei et al., 2007, 2008; Saleem et al., 2010, 2011a; Deka and Joy, 2007). A similar fact has been corroborated in the XRD patterns of all synthesized compositions as represented in Fig. 1. The partial co-substitution of Fe and Al does not disturb the wurtzite crystal structure with  $\text{P6}_3\text{mc}$  space group of parent ZnO, as diffraction peaks in all compositions were absolutely indexed. However, the lower intensity, broadening and shifting of diffraction peaks are attributed to the doping effects and difference in ionic radii of Zn (0.74 Å), Fe (0.63 Å) and Al (0.535 Å) atoms Saleem et al. (2011a) and Dinesha et al. (2009). The lattice parameters 'a' and 'c' of the synthesized DMS compositions were calculated using the 'CELL' software (Saleem et al., 2011a), which provides a very convenient and reliable way of measurement for quite complex wurtzite hexagonal like crystal structures. The lattice parameters 'a' and 'c', were found to vary from 3.2282 to 3.2512 Å and 5.2311 to 5.2466 Å, respectively, with the increase of Al content, as shown in Fig. 2. The breadth of the XRD characteristic peaks associated with the full width half maximum (FWHM) values observed was significantly much higher in Al doped compositions which indicated the lower size of crystallites. The estimated crystallite size of all compositions has been calculated using Scherrer relations (Pei et al., 2008) by

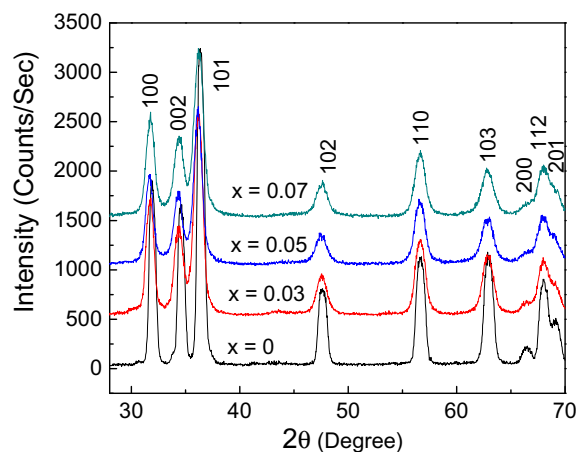


**Figure 1** XRD spectra of  $\text{Zn}_{0.95}\text{Fe}_{0.05}\text{Al}_x\text{O}$  ( $x = 0, 0.03, 0.05, 0.07$ ) samples.

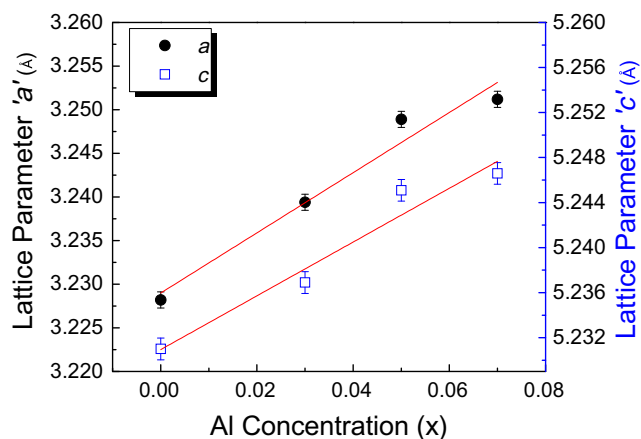


**Figure 2** Variation of lattice constants 'a' and 'c' with the increase of Al content.

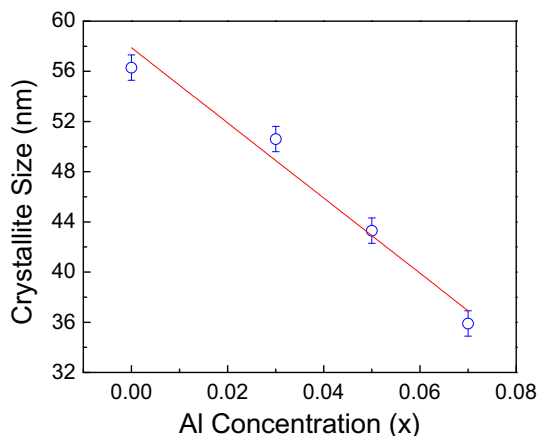


**Figure 3** Variation of crystallite size with the increase of Al content.

considering the position and broadening of most intense characteristic diffraction peak (101). The evaluated crystallite size of Mn doped ZnO sample was found at 56.3 nm, which was decreased to 35.9 nm with an increase in Al content up to  $x = 0.07$  as shown in Fig. 3.

### 3.2. Morphological analysis

Fig. 4a and b represents the SEM micrographs of  $\text{Zn}_{0.95}\text{Fe}_{0.05}\text{Al}_x\text{O}$  ( $x = 0, 0.07$ ) nanocrystallite compositions. The grains appeared in various shapes and sizes in both micrographs. There are no sharp and clear boundaries indicated in morphologies. However, it can be observed that the size of the grains is obviously smaller in the Al doped composition which indirectly supports the XRD measurements.

### 3.3. Electrical resistivity

The dc electrical resistivity of pelletized DMS compositions  $\text{Zn}_{0.95}\text{Fe}_{0.05}\text{Al}_x\text{O}$  ( $x = 0, 0.03, 0.05, 0.07$ ) is expected to decrease by the partial substitution of  $\text{Al}^{3+}$  atoms at  $\text{Zn}^{2+}$  sites. The composition without the doping of Al content showed a maximum value of resistivity of  $7.79 \times 10^6 \Omega\text{-cm}$  as represented in Fig. 5. It was found that electrical resistivity decreased with the increase of the doping content of Al. The lowest values of resistivity were found in the composition doped with maximum Al content ( $x = 0.07$ ). This trend might be attributed to the increase of concentration of free carriers (electrons) in the structure. The overall behavior of electrical resistivity observed in all the synthesized compositions was that the resistivity values reduced with the increase of temperature revealing the semiconducting nature of DMSs.

### 3.4. Magnetic properties

Fig. 6 represents the room temperature field dependent magnetic hysteresis (M-H) loops of  $\text{Zn}_{0.95}\text{Fe}_{0.05}\text{Al}_x\text{O}$  ( $x = 0, 0.03, 0.05, 0.07$ ) DMS compositions which clearly indicate the existence of ferromagnetic interactions. The partial substitution of Fe ions at the regular Zn sites could be attributed to this ferromagnetism. The origin of ferromagnetism in ZnO based DMS materials has remained controversial from the last decade. It was observed in XRD analysis that Fe and Al atoms successfully substitute the regular Zn sites. As no clusters or secondary phases were detected in XRD patterns, the option of the rise of ferromagnetism due to these phases can be eliminated. In addition, ZnO has natural n-type conductivity. Therefore, introduction of ferromagnetic interactions because of hole mediated Zener field model could not be possible. According to RKKY theory (Sharma et al.,

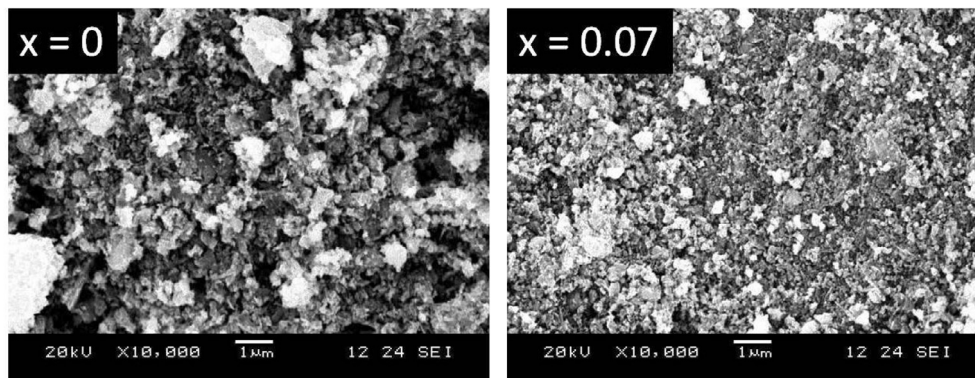


**Figure 4** SEM micrographs of  $\text{Zn}_{0.95}\text{Fe}_{0.05}\text{Al}_x\text{O}$  ( $x = 0, 0.07$ ) samples.

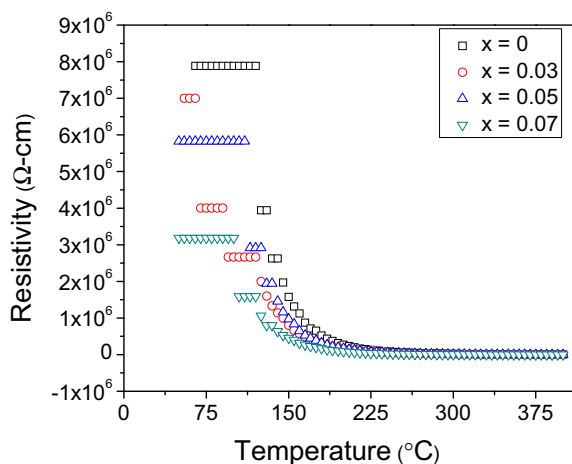


**Figure 5** Temperature dependent DC electrical resistivity of  $Zn_{0.95}Fe_{0.05}Al_xO$  ( $x = 0, 0.03, 0.05, 0.07$ ).

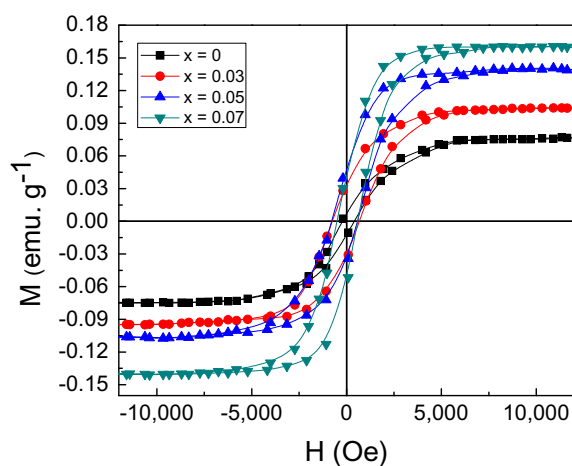


**Figure 6** Field dependent M-H loops of  $Zn_{0.95}Fe_{0.05}Al_xO$  ( $x = 0, 0.03, 0.05, 0.07$ ) samples.

2007; Priour et al., 2004) about ferromagnetism in ZnO based DMS materials, the exchange interaction between local spin-polarized electrons (such as the electrons of  $Fe^{2+}$  ions) and conductive electrons was the main cause of magnetism. The presence of free carriers has a considerable importance for the appearance of ferromagnetic behavior in Fe doped ZnO. In addition, it appears that Al doping affects the concentration of carriers in the structure, which are responsible for the establishment of magnetic phase. Consequently, the value of saturation magnetization ( $M_s$ ) obtained from the M-H loops was observed to increase from a value of 0.077–0.160 emu/g, with the increase of Al content up to  $x = 0.07$ . Hence, the additional doping of Al in ZnO based DMS materials significantly enhances the concentration of carriers which plays its vital role in magnetic phase establishment through carrier mediated RKKY exchange interactions.

#### 4. Conclusion

$Zn_{0.95}Fe_{0.05}Al_xO$  ( $x = 0, 0.03, 0.05, 0.07$ ) nanocrystallites of DMSs was successfully synthesized in phase pure form using sol gel derived auto combustion technique. Wurtzite type

hexagonal crystal structure was detected in all compositions. It was observed that lattice parameters, crystallite size and electrical resistivity varied with the doping of Al. The decrease of resistivity with the rise of temperature attributed to the semiconducting nature of materials. The concentration of free carriers was observed to increase with the increase of Al content which enhanced magnetization through carrier mediated mechanism. It is concluded that carrier mediated RKKY exchange interactions are mainly responsible for ferromagnetism in ZnO based DMS materials.

#### Acknowledgement

The Authors extend their appreciation to the Deanship of Scientific Research at King Saud University for funding the work through the research group project No RGP-VPP-106.

#### References

- Ahmed, F., Kumar, S., Arshi, N., Anwar, M.S., Koo, B.H., Lee, C.G., 2011a. Rapid and cost effective synthesis of ZnO nanorods using microwave irradiation technique. *Funct. Mater. Lett.* 4, 1–5.
- Ahmed, F., Kumar, S., Arshi, N., Anwar, M.S., Koo, B.H., Lee, C.G., 2011b. Defect induced room temperature ferromagnetism in well-aligned ZnO nanorods grown on Si (100) substrate. *Thin Solid Films* 519, 8199–8202.
- Ahmed, F., Kumar, S., Arshi, N., Anwar, M.S., Koo, B.H., Lee, C.G., 2012a. Doping effects of  $Co^{2+}$  ions on structural and magnetic properties of ZnO nanoparticles. *Microelectron. Eng.* 89, 129–132.
- Ahmed, F., Kumar, S., Arshi, N., Anwar, M.S., Koo, B.H., 2012b. Morphological evolution between nanorods to nanosheets and room temperature ferromagnetism of Fe-doped ZnO nanostructures. *Cryst. Eng. Commun.* 14, 4016–4026.
- Coe, J.M.D., Douvalis, A.P., Fitzgerald, C.B., Venkatesan, M., 2004. Ferromagnetism in Fe-doped  $SnO_2$  thin films. *Appl. Phys. Lett.* 84, 1332–1334.
- Coe, J.M.D., Venkatesan, M., Fitzgerald, C.B., 2005. Donor impurity band exchange in dilute ferromagnetic oxides. *Nat. Mater.* 4, 173–179.
- Deka, S., Joy, P.A., 2007. Synthesis and magnetic properties of Mn doped ZnO nanowires. *Solid State Commun.* 142, 190–194.
- Dinesha, M.L., Jayanna, H.S., Ashoka, S., Chandrappa, G.T., 2009. Temperature dependent electrical conductivity of Fe doped ZnO nanoparticles prepared by solution combustion method. *J. Alloys Compd.* 485, 538–541.
- Fukumura, T., Yamada, Y., Oyosaki, H.T., Hasegawa, T., Koinuma, H., Kawasaki, M., 2004. Exploration of oxide-based diluted magnetic semiconductors toward transparent spintronics. *Appl. Surf. Sci.* 223, 62–67.
- Gupta, A., Cao, H., Parekh, K., Rao, K., Raju, A., Waghmare, U., 2007. Room temperature ferromagnetism in transition metal (V, Cr, Ti) doped  $In_2O_3$ . *J. Appl. Phys.* 101, 09N513.
- Hong, N.Y.H., Sakai, J., Hassini, A., 2004. Ferromagnetism at room temperature with a large magnetic moment in anatase V-doped  $TiO_2$  thin films. *Appl. Phys. Lett.* 84, 2602–2604.
- Kim, J.H., Kim, H., Kim, D., Ihm, Y.E., Choo, W.K., 2002. Magnetic properties of epitaxially grown semiconducting  $Zn_{1-x}Co_xO$  thin films by pulsed laser deposition. *J. Appl. Phys.* 92, 6066–6071.
- Park, J.H., Kim, M.G., Jang, H.M., Ryu, S., 2004. Co-metal clustering as the origin of ferromagnetism in Co-doped ZnO thin films. *Appl. Phys. Lett.* 84, 1338–1340.
- Pearton, S.J., Norton, D.P., Ip, K., Heo, Y.W., Steiner, T., 2005. Recent progress in processing and properties of ZnO. *Prog. Mater. Sci.* 50, 293–340.

- Pei, G., Xia, C., Wang, L., Li, X., Jiao, X., Xu, J., 2007. Synthesis and characterizations of Al-doped  $\text{Zn}_{0.95}\text{Ni}_{0.05}\text{O}$  nanocrystals. *Scripta Mater.* 56, 967–970.
- Pei, G., Wu, F., Xia, C., Zhang, J., Li, X., Xu, J., 2008. Influences of Al doping concentration on structural, electrical and optical properties of  $\text{Zn}_{0.95}\text{Ni}_{0.05}\text{O}$  powders. *Curr. Appl. Phys.* 8, 18–23.
- Priour Jr., D.J., Hwang, E.H., Sarma, S.D., 2004. Disordered RKKY lattice mean field theory for ferromagnetism in diluted magnetic semiconductors. *Phys. Rev. Lett.* 92, 117201–117204.
- Saleem, M., Siddiqi, S.A., Atiq, S., Anwar, M.S., Riaz, S., 2010. Room temperature magnetic behavior of Sol–Gel synthesized Mn doped ZnO. *Chin. J. Chem. Phys.* 23, 469–472.
- Saleem, M., Siddiqi, S.A., Atiq, S., Anwar, M.S., Hussain, I., Alam, S., 2011a. Carriers-mediated ferromagnetic enhancement in Al-doped ZnMnO dilute magnetic semiconductors. *Mater. Charact.* 62, 1102–1107.
- Saleem, M., Siddiqi, S.A., Atiq, S., Anwar, M.S., 2011b. Structural and magnetic studies of  $\text{Zn}_{0.95}\text{Co}_{0.05}\text{O}$  and  $\text{Zn}_{0.90}\text{Co}_{0.05}\text{Al}_{0.05}\text{O}$ . *Chin. Phys. Lett.* 28, 116103.
- Saleem, M., Atiq, S., Naseem, S., Siddiqi, S.A., 2012. Structural and magnetic studies of Ni-doped ZnO synthesized with auto-combustion and co-precipitation techniques. *J. Korean Phys. Soc.* 60, 1772–1775.
- Sharma, V.K., Xalxo, R., Varma, G.D., 2007. Structural and magnetic studies of Mn-doped ZnO. *Cryst. Res. Technol.* 42, 34–38.
- Tong, L.N., He, X.M., Han, H.B., Hu, J.L., Xia, A.L., Tong, Y., 2010. Effects of  $\text{H}_2$  annealing on ferromagnetism of Ni-doped ZnO powders. *Solid State Commun.* 150, 1112–1116.
- Venkatesan, M., Fitzgerald, C.B., Lunney, J.G., Coey, J.M.D., 2004. Anisotropic ferromagnetism in substituted Zinc Oxide. *Phys. Rev. Lett.* 93, 177206–177209.
- Wolf, S.A., Awschalom, D.D., Buhrman, R.A., Daughton, J.M., Molnar, S.V., Roukes, M.L., 2001. Spintronics: a spin-based electronics vision for the future. *Science* 294, 1488–1495.
- Yang, J.H., Zhao, L.Y., Ding, X., Yang, L.L., Zhang, Y.J., Wang, Y.X., Liu, H.L., 2009. Magnetic properties of Co-doped ZnO prepared by sol–gel method. *Mater. Sci. Eng. B* 162, 143–146.
- Yu, Z., Ge, S., Zuo, Y., Wang, G., Zhang, F., 2010. Vacancy-induced room-temperature ferromagnetism in ZnO rods synthesized by Ni-doped solution and hydrothermal method. *Appl. Surf. Sci.* 256, 5813–5817.